

Quantitative visualization of the development of the blast structure generated by a 0.5 g-PETN pellet using background-oriented schlieren within an explosion chamber

Toshiharu Mizukaki^{*†}, Yoshito Hayakawa^{**}, Tomoharu Matsumura^{***},
Kunihiko Wakabayashi^{***}, and Yoshio Nakayama^{***}

^{*}School of Engineering, Tokai University, 4-1-1, Kitakaname, Hiratsuka, Kanagawa 259-1292, JAPAN
Phone : +81-463-58-1211

[†]Corresponding author : mizukaki@keyaki.cc.u-tokai.ac.jp

^{**}Nippon koki Co., Ltd., 2-1, Aza-Habu, Oaza-Nagasaka, Saigo-Mura, Nishishirakawa-Gun, Fukushima 961-8686, JAPAN

^{***}National Institute of Advanced Industrial Science and Technology, Tsukuba-Chuo 5th, 1-1-1, Higashi, Tsukuba, Ibaraki 305-8565, JAPAN

Received : July 24, 2015 Accepted : July 14, 2016

Abstract

The present study describes the result of the application of a novel optical flow visualization method called background-oriented schlieren (BOS) for understanding the evolution of shockwaves generated by cylindrical explosives, in particular, a pentaerythritol tetranitrate (PETN) pellet with mass of 0.501 g, diameter of 7.63 mm, and length of 7.53 mm. The experiment was performed to demonstrate the advantages of BOS for the visualization of shockwaves inside a heavily sealed chamber without any installed optics including schlieren mirrors. In this case, the chamber used was a cocoon-shaped steel wall of approximately 5 m in diameter, 10 m in height, and 0.525 m in wall thickness. From outside the chamber through an observation window, a propagating shockwave was recorded by a high-speed video camera capable of capturing 50,000 frames per second, and visualized by BOS with random-dot pattern as a background. Numerical analysis with the commercial-hydro code ANSYS AUTODYN was performed to validate the diffraction angle reconstructed by BOS. The histories of propagated shockwaves of radii up to approximately 0.5 m revealed that the strong jet of the detonation-product gas discharged along the length-axis of the explosive drove the distorted shockwave, even at 30 times of the explosive's length. The value of the diffraction angle behind the shock front agreed well between experimental and numerical analysis. The present study has successfully shown that BOS is a suitable method for visualizing explosion related fluid phenomena inside a sealed chamber.

Keywords : background-oriented schlieren, flow visualization, high-speed imaging, blast wave structure, PETN

1. Introduction

Optical flow visualization techniques including schlieren and shadowgraph imaging have been widely used for shockwave visualization in explosion research. Optical flow visualization allows us to recognize the propagation of a shockwave, development of a flow field, and interaction

of a flow field with obstacles. Furthermore, using interferometry, one can obtain contours of values of interest.

In contrast, several limitations remain in cases in which one requires quantitative information. First, quantitative measurement requires beam collimation by optical

components at the test section. Next, the observation area must be equal to or smaller than the diameter of the optical component used to generate the collimated beam. Finally, at present, there are only few techniques to obtain quantitative fluid dynamical information, including density distributions, for open-air experiments.

The background-oriented schlieren (BOS) method, which is a synthetic visualization technique using digital image processing, has an advantage in terms of applicability to open-air experiments compared with ordinary optical flow visualization methods. Furthermore, the BOS method provides quantitative information including density distribution. The principle of the BOS method is based on the same one as ordinary but the process of visualization is totally different. The first attempt to apply the BOS method to a full-scale experiment for visualizing a blade vortex interaction (BVI), was made by Raffel *et al.*¹⁾ and Richard *et al.*^{2), 3)}, and involved examining a hovering helicopter at low altitude with a background pattern of white paint splashed on the ground. They validated the accuracy of this method by comparing its result with that of hot wire velocimetry. An attempt to use the BOS method for shockwaves generated by a large-scale explosion was also made by Sommersel *et al.*⁴⁾ The shockwave produced by the ignition of a hydrogen-air mixture gas inside a container was examined against a forest background. The overpressure profile obtained from the visualized images was compared with a numerical solution.

In the present study, quantitative visualization of an explosion generated by a sub gram order explosive with a detonator has been conducted to demonstrate the advantage of the BOS method against the ordinary ones. An explosion was made in an explosion chamber in which the optical components involved in conventional visualization methods were not installed. In general, practical limitations on quantitative or qualitative optical flow visualization exist in an explosion chamber; such limitations include optical access, installability of the optical components, and prevention of the optical components from sustaining damage from the explosion debris. The BOS method has revealed the direction-dependence of the propagation of the shock front, the peak overpressure profile, and applicability of the BOS method to the computed tomography (CT) method. The results shown in the present study indicate that the BOS method is an expansive diagnostic technique for the explosion research field.

2. Background-oriented schlieren

BOS has been proposed for visualization of flows with density change for a decade. Its principle is simple and easy to conduct with a commercial off-the-shelf apparatus. From the optics viewpoint, the BOS method is a form of white light speckle photography similar to the laser-speckle method, except that a white light source is used to record instead of a laser. However, from the image-processing viewpoint, the BOS method uses a principle similar to particle image velocimetry (PIV), except that

PIV uses micro-particles such as oil mist or dust in the air to detect flow. In contrast, the BOS method uses the background pattern, including random dots, behind the test section.

In 1998, Meier⁵⁾ proposed a visualization technique to provide the density distribution within a phase phenomenon of interest by detecting and analyzing the distribution of the background pattern displacement using digital image processing. The method was called the BOS method or background-oriented-optical tomography (BOOT). The principal advantage of this technique, in comparison with other density-recording optical techniques such as the shadowgraph, schlieren, speckle, and interferometry methods, was its extremely modest technical requirements, usually only one (electronic) camera, a sufficiently structured background, and a PC. The reason this technique had not been applied earlier was probably because of the requirement for fast and accurate de-convolution algorithms, which had only recently become available for PCs.

Another advantage of the BOS method is its unlimited field of view, and consequently, its capacity to monitor objects of unlimited size⁶⁾. Because of the typically conical viewing field of the camera used, the size of any phase object can be matched by distance and focal length. In contrast, the conical shape of the projection and the different sensitivities of the spatially-distributed schlieren necessitate certain correction and calibration procedures. An additional difficulty is the need for focusing on the background and schlieren simultaneously. This can be achieved by a small aperture and short distance between the background and schlieren. The use of telocentric beams for this purpose is prohibited by the requirement, in most applications of large lenses or mirrors. The optimal sensitivity and resolution of the device are achieved when the background structure has a texture close to the camera resolution.

Figure 1 shows the principle of the BOS method. Since the refraction of a single beam contains information about the spatial gradient of the refractive index integrated along the axial path, the image refraction angle, ϵ is defined as⁷⁾ follows :

$$\epsilon = \frac{1}{n_0} \int_{Z_D - \Delta Z_D}^{Z_D + \Delta Z_D} \frac{\delta n}{\delta y} dZ \quad (1)$$

with the assumption that the half-width of the region of the density gradient, ΔZ_D , is significantly smaller than the distance between the region of the density gradient and the background, Z_D , : $\Delta Z_D \ll Z_D$. In Equation (1), n_0 indicates the refraction index of the reference condition. Furthermore, it is seen from the geometry that the virtual image displacement is related to the image displacement by the lens distance from the background, Z_B , and the image distance from the lens, Z_i , which for large Z_B can be replaced by the focal length, f , of the lens as follows :

$$\frac{\Delta Y}{Z_B} = \frac{\Delta y}{Z_i} = \frac{\Delta y}{f}. \quad (2)$$

For small deflection angles, ϵ can be approximated as

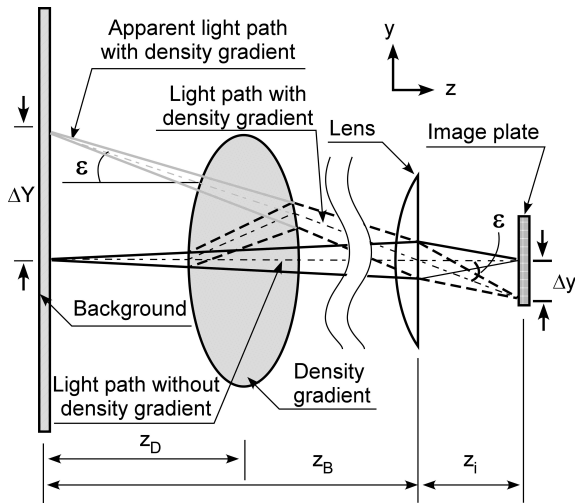


Figure 1 Principle of background-oriented schlieren.

follows :

$$\Delta y = z_D M \epsilon, \tag{3}$$

where $M = z_i/z_B = f/z_B$. Hence,

$$\epsilon = \frac{z_B \Delta y}{z_D f}. \tag{4}$$

The magnitude of the background displacement on the obtained image of the shockwave was provided by an image-matching algorithm based on the cross-correlation function between the target image and the reference image. After this magnitude was determined, the refraction angle, ϵ , of the light passing through the spherical shock was determined using Equation (3). The density distribution behind the shock front was not reconstructed in this study because the explosions and background were observed from only one direction for each experiment and the magnitude of the displacement of the hidden area due to the combustion products of the explosion was not obtained. A two-dimensional reconstruction method such as the Abel transform⁸⁾ does not function properly when information about the target phenomenon is missing. Simultaneous observations from multiple directions made with a computed homographic technique can reconstruct the density distribution behind the shock front, even if the combustion products hide the background near the explosion center.

3. Experimental and numerical methods

3.1 Explosives

A pentaerythritol tetranitrate (PETN) pellet with a mass of 0.50 g, diameter of 7.63 mm, and length of 7.53 mm was used as an energy source for shockwave-generation. The PETN pellet was ignited with a detonator attached to one of its bottom surfaces. The detonator was ignited by a high voltage of 4 kV. The PETN pellet with the detonator was pasted onto a tensioned nylon string installed at the center of the explosion chamber. Figure 2 illustrates the configuration of the installation of the explosive inside the explosion chamber.

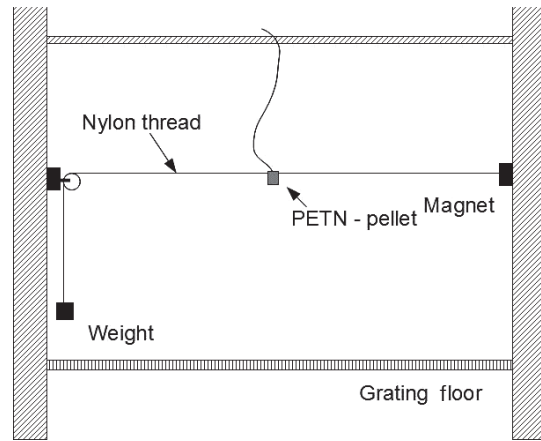


Figure 2 Installation of PETN in the explosion chamber.

3.2 Visualization method

Figure 3 shows the experimental setup for the visualization of shockwaves by BOS inside the explosion chamber. This chamber was a sealed cylindrical room five meters in diameter, bounded by a concrete wall with steel liner that was totally 0.525 m thick. A high-speed video camera (image size: 512 by 512 pixels; frame rate: 20,000 frames per second; exposure time: 1 μ s; Vision Research Phantom V1610) was placed outside the explosion chamber at a distance of $z_B = 6,275$ mm from the background screen (BS). A camera lens, L, with an 80-mm focal length and an F-number of F/2.8 was used as an imaging lens. Images were recorded through one of four optical accesses (OA) each of which had circular-thick window glass and a diameter of 150 mm. The PETN pellet, EX, was placed at the center of the explosion chamber at a height of 0.9 m from the grating floor (GF) (Figure 3). The EX was ignited with a detonator activated by a high-voltage trigger signal. The background screen, which was a 900 mm by 900 mm paper sheet with a random-dot pattern, BS, was placed at $z_D = 2,195$ mm from EX. The BS was illuminated with two strobe lights (duration: 2 ms, Panasonic) during recording. Image recording with HC was started at 100 μ s before sending the trigger signal to the detonator. The image before ignition was used as the reference image, which recorded the flow field without disturbances.

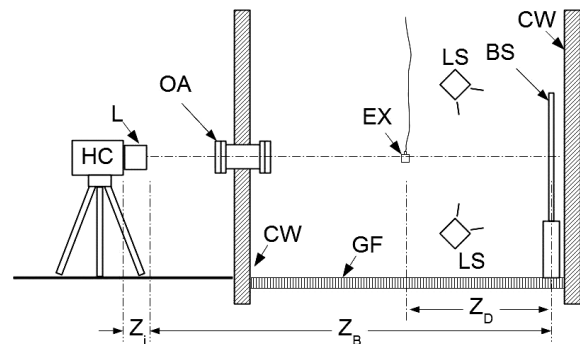


Figure 3 Experimental configuration of a shockwave-visualization system inside the explosion chamber; HC, high-speed-video camera; L, camera lens; CW, concrete wall; GF, grating floor; EX, PETN-pellet; LS, light source.

4
1
2

3.3 Numerical method

Numerical calculation was conducted to evaluate the propagation and density distribution caused by the explosion of a PETN-pellet. A hydro-code ANSYS AUTODYN⁹⁾ was used for this study. The computational domain is shown in Figure 4.

The fundamental equations governing the compressible time-dependent inviscid flow can be written in Cartesian coordinates as follows :

$$\begin{aligned} \frac{\partial \rho}{\partial t} + \frac{\partial}{\partial x_i}(\rho v_i) &= 0, \\ \frac{\partial v_i}{\partial t} + v_i \frac{\partial v_i}{\partial x_j} &= -\frac{1}{\rho} \frac{\partial p}{\partial x_j}, \\ \frac{\partial e}{\partial t} + v_i \frac{\partial e}{\partial x_j} &= -\frac{1}{\rho} \frac{\partial}{\partial x_j}(p v_i), \\ p &= p(\rho, e), \end{aligned}$$

where v_i , p , and ρ are the velocity component, pressure, and density of the fluid, respectively, and e is the specific total energy.

An explosion is considered as a sudden release of energy. In general, after detonation, the solid explosive is transformed into gaseous products that are initially at an extremely high pressure exceeding 100,000 atm. This high pressure is transformed into mechanical work by momentum transfer in the form of pressure waves, which propagate through the surrounding medium. In this study, we modeled the pressure-volume-energy behavior of the detonation-product gases of PETN with the standard Joes-Wilkins-Lee (JWL) equations¹⁰⁾ of state. The equations can be written as follows :

$$\begin{aligned} p &= A \left(1 - \frac{\omega}{AV}\right) e^{-R_1 V} + B \left(1 - \frac{\omega}{R_2 V}\right) e^{-R_2 V} + \frac{\omega E}{V}, \\ p_s &= A e^{-R_1 V} + B e^{-R_2 V} + C V^{-(\omega+1)}, \\ E_s &= \frac{A e^{-R_1 V}}{R_1} + \frac{B e^{-R_2 V}}{R_2} + \frac{C}{\omega V^\omega}, \end{aligned}$$

where V is the dimensionless specific volume of the detonation products from the specific volume of undetonated explosive, E is the internal energy per unit volume, and A , B , C , ω , R_1 , and R_2 are constants whose values are calculated using the Kihira-Hikita-Tanaka (KHT) equation¹¹⁾ of state. The parameters for PETN are given in Table 1.

The air was modeled as an ideal gas, which follows the gamma-law equation as follows :

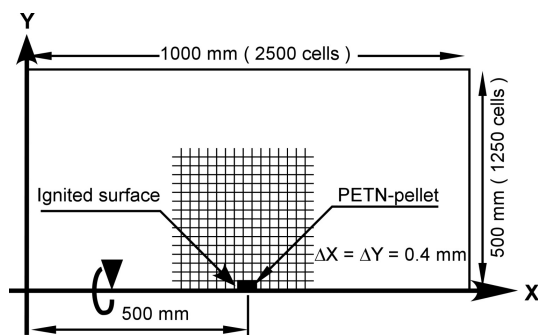


Figure 4 Computational domain for a PETN-pellet explosion.

Table 1 JWL parameter of PETN.

Parameter	Value	Unit	Parameter	Value	Unit
ρ_0	1.500×10^3	kg m^{-3}	V_{C-J}^*	7.450×10^3	m s^{-1}
A	6.253×10^2	GPa	E_{C-J}^*	8.560×10^6	kJ m^{-3}
B	2.329×10^1	GPa	P_{C-J}^*	2.200×10^1	GPa
R_1	5.250×10^0	None			
R_2	1.600×10^0	None			
ω	2.800×10^{-1}	None			

*1) V_{C-J} , C-J velocity

*2) E_{C-J} , C-J energy per unit volume

*3) P_{C-J} , C-J pressure.

$$p = (\gamma - 1) \frac{\rho}{\rho_0} E,$$

where $\gamma = 1.4$ is the ratio of the specific heats, ρ is the density of air, $\rho_0 = 1.20 \text{ kg m}^{-3}$ is the initial density, and E is the specific internal energy. To satisfy the standard atmospheric pressure, the initial value for the internal energy is set to $E = 2.50 \times 10^5 \text{ N m}^{-2}$.

4. Results and discussion

4.1 Overview of developing shockwaves

Figure 5 shows an overview of the development history of the blast waves caused by a 0.5-g PETN pellet. On each row, the high-speed image, numerical result of the pressure distribution, and background displacements of the horizontal and vertical components are shown from left to right at 200, 400, and 600 microseconds following ignition.

In the high-speed images, only the combustion gas around the explosion center (EC) was determined by visual inspection because none of the typical optics of conventional optical flow visualization techniques were used. The human eye can detect disturbances of the random dot background caused by the incident shockwave (IS) propagating for outbound and by strong vortices around the EC.

The numerical result indicated that the IS had a distorted shape caused by a higher propagation velocity along the negative y-axis than other directions. The faster propagation velocity was driven by a combustion gas jet (CJ) ejected by the end wall of the PETN-pellet along the negative y-axis. In Figure 5b, the secondary shock (SS) that was driven by the IS's constriction due to pressure decreasing by rapid expansion appears clearly behind the IS. The distorted shape maintained until 400 μs on numerical result.

The second and the third columns indicate background displacement (BOS images). The background displacement was determined by cross-correlation analysis on the measured images and the reference recorded before ignition. In the cross-correlation analysis, the size of the interrogation window was eight by eight pixels at the final stage. Each pixel had a two-dimensional displacement vector in sub-pixels in the x and y directions.

The second column shows the map of background

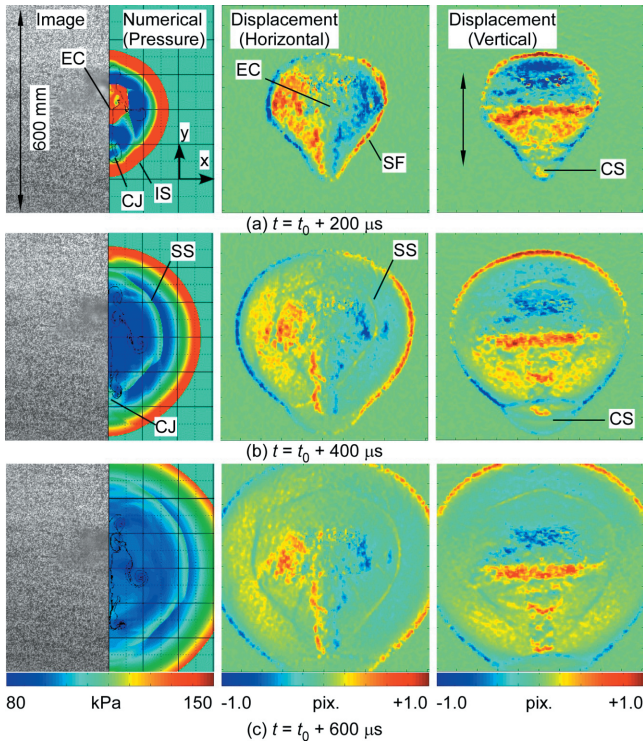


Figure 5 Shockwave development by high-speed-video camera, numerical analysis, and BOS.

displacement along the horizontal x-axis, and the third along the vertical y-axis. The colors on the map indicate the background displacement in the pixel and the sign indicates the direction of displacement, which is positive for the right-hand or upside, and negative for the left-hand or down side. The interpretation of the obtained image here is the same for the images obtained by the ordinary schlieren method with vertical and horizontal knife-edge positions.

The BOS images have clearly revealed the characteristics of the shockwaves caused by a PETN-pellet ignited with a detonator. In the early stage of the explosion, Figure 5a and b, the ISs were significantly distorted along CJ. By CJ, the bottom of IS was accelerated much more intensely than the other portion. The BOS image in the horizontal direction shows the development of CJ clearly. Finally, the outstanding shockwaves caused by CJ have formed a cell structure (CS) inside the IS. BOS images in the vertical direction show the development of the CS clearly. A secondary shockwave (SS) has clearly appeared in Figure 5b. SS has also been distorted by CJ. The magnitude of distortion related to CJ has been rapidly moderated with the propagation of IS up to 1 ms.

4.2 r-t Diagram

To discuss the development of the IS initiated by the PETN-pellet with a detonator, radius (r) versus time (t) diagrams of the IS were made using BOS images and numerical analysis. On the BOS images, the radius of IS was determined to be the distance from the explosion center toward each direction at each moment. Figure 6 shows the r-t diagram. Lines indicate the results of numerical analysis and dots indicate those of the BOS image. The r-t diagrams in three directions-zero degrees,

90 degrees, and 180 degrees from y-axis-are examined here.

The r-t diagram in the propagation direction of zero degrees (Δ , experimental; broken line, numerical result in Figure 6): from the curve plotted, it can be seen that the IS propagated markedly more slowly than the numerical result. The experimental IS arrived at points 200 mm and 300 mm from the center of the explosion approximately 100 μ s and 150 μ s, respectively, later than it did in numerical simulation. A low propagation speed may have been produced by the negative pressure and the flow generated by the vortex surrounding the pellet axis inside the IS. The vortex will be discussed later. Another reason for this discrepancy was that the numerical analysis employed non-viscous momentum equations, Euler's equations, for fluid analysis. A non-viscous assumption causes shock fronts to propagate faster than they do in a physical situation. Therefore, the behavior of the IS along this direction, zero degrees, would provide less peak-overpressure than the IS propagated toward other directions.

The r-t diagram in the propagation direction of 90 degrees (\circ , experimental; short-broken line, numerical result in Figure 6): from ignition through the end of the recorded duration, the numerical and experimental results for arrival time agreed within 10 μ s at all locations. The IS in the experimental results propagated slightly more slowly than in the numerical results. This result indicated that the shockwave propagation at 90 degrees was less affected by the CJ because of moving perpendicularly to the pellet axis. Therefore, the behavior of the IS propagating at 90 degrees was easy to predict and showed good agreement with experimental results.

The r-t diagram in the propagation direction of 180 degrees (\square , experimental; solid line, numerical result in Figure 6): by 100 μ s after ignition, the IS had rapidly propagated up to approximately 220 mm, whereas the IS in the computational domain reached the same radius at 200 μ s. The rapid propagation toward 180 degrees caused strongly distorted shock front followed by the CJ. In the computational domain, the CJ appeared but did not make a significant difference compared with other directions. Beyond 300 μ s after ignition, the IS reduced its propagation velocity and finally reached almost zero velocity; i.e., it became parallel to the vertical (t)-axis. This phenomenon indicated deflation and re-expansion of the IS. The computational result indicated that deflation and re-expansion progressed from 420 μ s to 600 μ s. In this direction, the IS was rapidly accelerated by the CJ after ignition, and subsequently, decelerated down to nearly zero during recession process. Therefore, the shape of IS was strongly distorted up to approximately 300 mm from the explosion center.

4.3 Peak overpressure profile

To validate the applicability of BOS measurements for peak overpressure detection, peak overpressure profiles provided by both BOS measurement and numerical calculation are compared. Figure 7 shows the profiles of

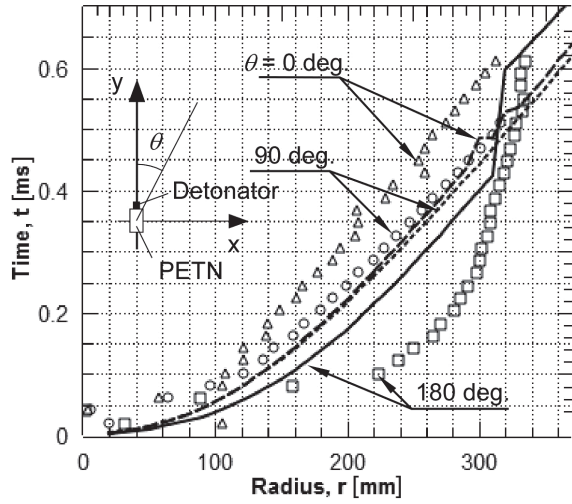


Figure 6 Direction dependence of the r - t diagram by experimental and numerical results.

the peak overpressure ratios, $\Delta p/p_0$ (where Δp and p_0 are overpressure and initial pressure, respectively), for both experimental and numerical results for propagation directions of 90 and 180 degrees. To obtain a peak overpressure ratio, the following process was conducted. First, to determine the IS velocity at each frame, U_s , the travel distance of IS at the inter frame was divided by interval time, $20.4 \mu\text{s}$ (49008 fps). Then the Mach number, M_s , was obtained by dividing U_s by the speed of sound, $a_0 = (\gamma RT)^{1/2}$ [12], where γ , R , and T are the specific heat ratio of air, 1.4, the gas constant for air, $287.1 \text{ J kg}^{-1} \text{ K}^{-1}$, and temperature, 288 K, respectively. Finally, the peak overpressure ratio, $\Delta p/p_0$, was determined by calculation using^[13] the following equation :

$$\frac{\Delta p}{p_0} = \frac{2\gamma(M_s^2 - 1)}{\gamma + 1} = \frac{7(M_s^2 - 1)}{6},$$

where the term to the right applies if $\gamma = 1.4$.

With regard to the propagation direction of 90 degrees, the experimental result was approximately 70%-50% less than the numerical value at the same radius up to 100 mm, and then similar from 100 mm to 200 mm. Beyond a 200 mm radius, the values were scattered widely by increasing error because the incident shock Mach number approached unity. On the other hand, with regard to the propagation direction of 180 degrees, the experimental result was approximately 280%-50% larger than the numerical value at distances up to 200 mm. Beyond a 200 mm radius, the values were scattered widely by increasing error because the incident shock Mach number approached unity. These results indicate that the accuracy of extracted information from recorded images strongly depended on the spatial resolution of the image recording device used.

4.4 Density gradient and refraction angle inside the shock front

According to the principle of BOS, the background displacement caused by the phenomena observed represents the integral of the density gradient or index of refraction along the light path through those phenomena.

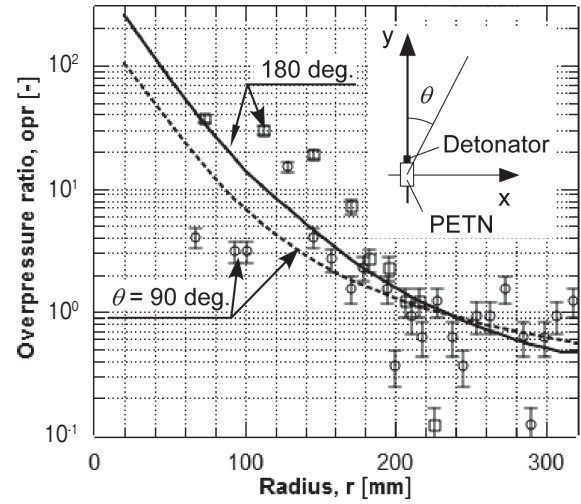


Figure 7 Direction dependence of the overpressure profile by experimental and numerical results.

Therefore, in the case of axisymmetric phenomena, the obtained BOS image represents the integrated information of its fluid structure. Theoretically speaking, once we obtain the background displacement map, the fluid dynamic structure could be revealed by applying a computed tomography technique to the map. On the other hand, the explosion instantaneously and drastically changed the flow field with heat discharge that would significantly disturb any efforts to obtain a clear image of the fluid dynamic structure using BOS measurement. In this section, to determine the duration time when a strong disturbance remained inside the shock front, an experimentally obtained background displacement map was compared with a numerically obtained one. Figure 8 shows the map of the background displacement through the shockwaves caused by a PETN-pellet up to $600 \mu\text{s}$ after ignition. The left half of each figure shows the experimental result and the right half shows the numerical one.

Figure 8a: $100 \mu\text{s}$ after ignition, an IS was strongly distorted by a CJ that was discharged from the side of the pellet opposite of that to which the detonator was attached, in this case, downward. The IS in the experimental result had a stronger distortion than the numerical. Figures 8b and c: $200 \mu\text{s}$ and $300 \mu\text{s}$ after ignition, the IS propagated outward and gradually became a spherical shockwave. On the other hand, the interior structure was not clear because of strong turbulence and heat effects. Figure 8d: $400 \mu\text{s}$ after ignition, except near the CJ region, the IS became a spherical shockwave. A secondary shockwave (SS) was generated after recession of the spherical shockwave. A strong vortex ring (V) appeared in the middle portion of the spherical shock. V was considered to be driven by CJ. Figure 8e and f: $500 \mu\text{s}$ and $600 \mu\text{s}$ after ignition, the flow field structure was clearly visualized, including the IS, SS, CJ, and CJ-driven vortex ring.

Based on the description above, we determined that the BOS technique was capable of reconstructing flow structures inside spherical shocks generated by a 0.50-g PETN pellet with a cylindrical shape under this

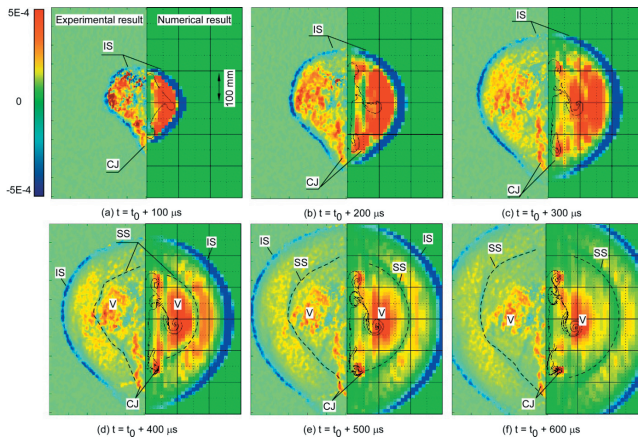


Figure 8 Comparison of the density gradient inside the incident shockwave between BOS and numerical analysis.

experimental configuration.

5. Summary

To visualize the early stages of an explosion caused by a 0.5-g PETN pellet in an explosion chamber with no optical components including schlieren mirrors, the BOS method using a high-speed video camera and a retro-reflective background was applied. The analyzed images recorded at a $50 \mu\text{s}$ interval and a $1 \mu\text{s}$ exposure time revealed the direction dependence of the shock front propagation, the peak overpressure profile, the density gradient distribution inside the shock front, the flow field structure development inside the shock front, and the applicability of BOS to computed tomography. Based on the result shown here, the authors have demonstrated that BOS has advantages for the visualization of explosions in explosion chambers where no optical components can be installed compared to conventional flow visualization methods that require parallel light to operate. Furthermore, three-dimensional flow-field analysis is promised by the BOS combined with a computed tomography method, CT-BOS.

Acknowledgement

The authors would like to express gratitude to Dr. Atsushi Abe and his colleagues of ITOCHU Techno-Solutions Corporation for their kind advice for numerical analysis.

References

- 1) M. Raffel, H. Richard, and G.E.A. Meier, On the applicability of background-oriented-optical tomography for large scale aerodynamic investigations, *Experiments in Fluids*, 28, 477–481 (2000).
- 2) H. Richard, M. Raffel, M. Rein, J. Kompenhans, and G.E.A. Meier, Demonstration of the applicability of a Background-Oriented Schlieren (BOS) method, 10th International Symposium on Applications of Laser Techniques to Fluid Mechanics Lisbon, (2000).
- 3) H. Richard and M. Raffel, Principle and applications of the background-oriented schlieren (BOS) method, *Measurement Science and Technology*, 12 pp.1576–1585 (2001).
- 4) O.K. Sommersel, D. Bjerketvedt, S.O. Christensen, O. Krest, and K. Vagsaether, Application of background-oriented schlieren for quantitative measurements of shock waves from explosions, *Shock Waves*, 18, 291–297 (2008).
- 5) G.E.A. Meier, “New optical tools for fluid mechanics”, Paper 226, 8th International Symposium on Flow Visualization, Sorrento 22, 6 (1998).
- 6) T. Mizukaki, T. Matsumura, K. Wakabayashi, and Y. Nakayama, Background-oriented schlieren with natural background for quantitative visualization of open-air explosions, *Shock Waves*, 24, 69–78 (2014).
- 7) W. Merzkirch, “Flow Visualization, 2nd ed”, Academic Press, Orlando, Florida (1987).
- 8) N. Fomin, “Speckle Photography for Fluid Mechanics Measurements”, Springer (1998).
- 9) M.S. Cowler, N.K. Birunbaum, M. Itoh, K. Katayama, and H. Obata, “AUTODYN-an interactive non-linear dynamic analysis program for microcomputer through supercomputers”, *Transactions of 9th International Conference on Structural Mechanics in Reactor Technology*, B 401–406 (1987).
- 10) B.M. Dobratz, and P.C. Crawford, “LLNL Explosives Handbook: Properties of Chemical Explosives and Explosive Simulants”, University of California; Lawrence Livermore National Laboratory, UCRL–52997, (1981).
- 11) K. Tanaka, “Detonation Properties of High Explosives Calculated by Revised Kihara-Hikita Equation of State,” *The Eighth International Detonation Symposium*, Albuquerque, New Mexico, 548–557 (1985).
- 12) H.W. Liepmann and A. Roshko, *Elements of Gasdynamics*, “John Wiley and Sons, New York (1957).
- 13) G.F. Kinney and K.J. Graham, “Explosive Shocks in Air, Macmillan”, New York (1962).